Roles of Electric Field Shear and Shafranov Shift in Sustaining High Confinement in Enhanced Reversed Shear Plasmas on the TFTR Tokamak

E. J. Synakowski, S. H. Batha,* M. A. Beer, M. G. Bell, R. E. Bell, R. V. Budny, C. E. Bush,† P. C. Efthimion, G. W. Hammett, T. S. Hahm, B. LeBlanc, F. Levinton,* E. Mazzucato, H. Park, A. T. Ramsey, G. Rewoldt, S. D. Scott, G. Schmidt, W. M. Tang, G. Taylor, and M. C. Zarnstorff

Princeton Plasma Physics Laboratory, Princeton, New Jersey 08543

(Received 24 October 1996)

The relaxation of core transport barriers in TFTR enhanced reversed shear plasmas has been studied by varying the radial electric field using different applied torques from neutral beam injection. Transport rates and fluctuations remain low over a wide range of radial electric field shear, but increase when the local $\mathbf{E} \times \mathbf{B}$ shearing rates are driven below a threshold comparable to the fastest linear growth rates of the dominant instabilities. Shafranov-shift-induced stabilization alone is not able to sustain enhanced confinement. [S0031-9007(97)02841-X]

PACS numbers: 52.55.Fa, 52.25.Fi, 52.35.Ra, 52.55.Dy

The possible role of the radial electric field in forming and sustaining transport barriers in H modes and VH modes has been discussed extensively [1–4]. TFTR enhanced reversed shear (ERS) [5] and DIII-D negative central shear (NCS) [6] plasmas possess transport barriers deep in the plasma core, and large values of the radial electric field E_r and its gradient have been associated with high confinement in these regimes [7,8]. However, it remains an open question whether E_r plays a causative role in reducing transport in these cases. Indeed, high core particle, energy, and momentum confinement obtained by any means will lead to increased pressures and velocities, and most likely to large values of E_r and ∇E_r.

While E_r plays a central role in proposed mechanisms for transport bifurcations and good confinement [9], other proposals have been made in which it is not involved [10,11]. The suggestion that E_r is the key in balanced-injection TFTR ERS plasmas takes the following form: central fueling and heating results in steep gradients in the plasma pressure p, which yield large gradients in E_r and the $\mathbf{E} \times \mathbf{B}$ flow shear [12,13]. With sufficiently large flow shear, turbulence is decorrelated. This leads to a reduction in transport, and to a further increase in ∇p and confinement. Low current density yields a large Shafranov shift Δ, and thus increased ∇p and $\mathbf{E} \times \mathbf{B}$ shear, as compared to plasmas with peaked current density profiles of the same stored energy. The alternative explanation for the formation of core transport barriers relies on the role of Δ itself. In Ref. [10], reduction of instability drives and the formation and sustainment of transport barriers is predicted for TFTR reversed shear plasmas as a result of favorable precession of barely trapped particles induced by large gradients in the Shafranov shift Δ'. Similar arguments were made examining ballooning-type instabilities in the plasma edge [11]. Proposals based on both $\mathbf{E} \times \mathbf{B}$ and Δ' effects suggest a combined picture in which growth rate reduction induced by large Δ' enables the $\mathbf{E} \times \mathbf{B}$ shear to be effective. In all of the above scenarios, good confinement is expected to be reinforced by the stabilization of ion-thermal-gradient turbulence from the peaking of the density profile [14].

Results presented in this Letter indicate that $\mathbf{E} \times \mathbf{B}$ shear effects are necessary, and that Shafranov shift effects are not sufficient, to maintain the observed low radial transport and fluctuation levels in ERS plasmas. Experimentally, it is difficult to separate the roles of $\mathbf{E} \times \mathbf{B}$ shear and Δ' effects. Since large values of E_r and ∇p accompany large Shafranov shifts, a means of varying E_r independent of ∇p is required to decouple the two effects. In these experiments, ERS plasmas were generated with similar neutral beam powers and heating profiles, which fixed quantities central to Δ'-induced stabilization. However, these plasmas had various applied torques and thus different degrees of toroidal velocity V_ϕ. For any plasma species, the radial force balance equation is given by $E_r = \nabla p/(nZe) + V_\phi B_\theta - V_\theta B_\phi$, where n is the density of the species in question, Z is the charge number, e is the electronic charge, V_θ is the poloidal rotation velocity, B_θ is the poloidal magnetic field, and B_ϕ is the toroidal field. Thus V_ϕ variations result in changes in E_r and its shear. In a toroidal geometry, the gradient in the quantity E_r/RB_θ characterizes the decorrelation rate of turbulence [13], where R is the major radius. On the outer midplane, the characteristic $\mathbf{E} \times \mathbf{B}$ shearing rate can be written as $\gamma_{\mathrm{E}\times\mathrm{B}} = E_r/B[1/E_r(\partial E_r/\partial R) - (1/B_\theta)\partial B_\theta/\partial R - 1/R]$ [15], where B is the total magnetic field magnitude. The causative role of E_r in sustaining enhanced confinement is in part indicated by the observation that core fluctuation and transport levels increase when $\gamma_{\mathrm{E}\times\mathrm{B}}$ is driven below a critical level, but remain low and unchanged above that threshold. This threshold behavior is anticipated in the work of Ref. [12]. In determining E_r, B_θ was measured with the motional stark effect diagnostic [16] before the

 0031-9007/97/78(15)/2972(4)$10.00

transition into the ERS regime, when contributions from the plasma E_r to the total electric field experienced by the beam neutrals were small [17]. After this time, the time-dependent transport code TRANSP [18] was used to calculate B_θ. V_ϕ and the carbon pressure p_c were measured with charge exchange recombination spectroscopy [19], and V_θ was calculated with the NCLASS code using the neoclassical treatment of Hirshman and Sigmar [20].

Plasmas with reverse magnetic shear were generated in the standard way [5] by heating them with a modest neutral beam power (7 MW) during the period of current ramp-up. Transitions to the ERS regime were obtained during a 350 ms period of high-power beam heating (28 MW) in a balanced configuration having nearly equal power injected tangentially parallel (co) and antiparallel (counter) to the plasma current. During this period the central electron density increased rapidly due to strong core particle fueling and improved core particle confinement, reaching $\sim 9 \times 10^{19}$ m^{-3} (Fig. 1). Favorable ERS confinement was sustained for variable durations in the subsequent "postlude" period of lower-power heating (14 MW), as indicated by the continued rise in central electron density. Six neutral beam sources were used in different combinations during the postlude phase, ranging from pure coinjection to predominantly counterinjection. This procedure varied V_ϕ, and thereby the $\mathbf{E} \times \mathbf{B}$ shear, while maintaining a constant Δ'.

The plasma pressure and pressure peakedness, total particle number, stored energy, Δ', and global energy confinement time remained nearly constant throughout the postlude period so long as the discharges remained in the ERS regime. Eventually, however, the core transport barrier was lost in some of the plasmas; they suffered a back transition to poorer confinement, indicated most simply by the decay in central electron density. There is a clear correlation between the applied beam torque and occurrence of such a back transition (Fig. 1). Counter-dominated, balanced, and slightly codominated injection sustained ERS confinement until the end of beam injection, but strongly codominated injection reproducibly triggered a back transition. Pure coinjection yielded the earliest confinement losses. Following back transitions, the electron particle diffusivity D_e increased by more than an order of magnitude in the region of previously good confinement, and the peaked electron profile density collapsed (Fig. 2). D_e was determined by a calculation of the particle source and electron flux Γ_e in the TRANSP code and is defined by $\Gamma_e \equiv -D_e \nabla n_e + V_{\mathrm{Ware}}$, where V_{Ware} is the Ware pinch.

The correlation of back transitions with varied applied torques at constant plasma pressure suggests that reductions in $\mathbf{E} \times \mathbf{B}$ shear are involved in the loss in ERS confinement. Increasing V_ϕ in the coinjection direction after the balanced phase leads to reductions in E_r and its gradient, as the change in the $V_\phi B_\theta$ term in the carbon radial force balance equation is of opposite sign compared to that of the ∇p_c and the $V_\theta B_\phi$ terms. Profiles of E_r and the components from the carbon force balance equation are shown in Fig. 3 for a corotating plasma at two times. The first time is shortly after the 28 MW balanced phase, and the second is in the earliest stages of the back transition. The local density and pressure at the latter time have just begun to fall. The ∇p_c and the $V_\theta B_\phi$ contributions to E_r are similar between these two times, but the magnitude and gradient of E_r are reduced significantly at the later time. While the local velocity shear increases as a result of coinjection, gyrokinetic simulations [21] indicate that it is far below that required to excite rotationally driven instabilities [22,23] which might cause a loss in confinement. The $V_\phi B_\theta$ term shown in Fig. 3 is negative in the outer half of the plasma, a result of the measured counterrotation present even with codominated injected power. NCLASS calculations indicate that the working ion V_ϕ is also counterdirected there. TRANSP analysis shows that this is consistent with the presence of a counterdirected torque, established by a radial current of thermal particles that arises to preserve ambipolarity in response to ripple loss of about 10% of

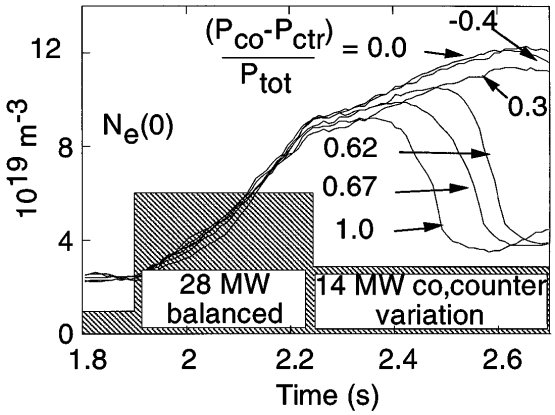

FIG. 1. The central electron density time evolution. Curves are labeled according to the difference on co- vs counterinjected power, $P_{\mathrm{co}} - P_{\mathrm{ctr}}$, divided by the total injected power P_{tot}. The shaded region indicates schematically the neutral beam heating wave form. The plasmas studied had a major radius of 2.60 m, a minor radius of 0.95 m, a toroidal magnetic field of 4.6 T, and a maximum plasma current of 1.6 MA.

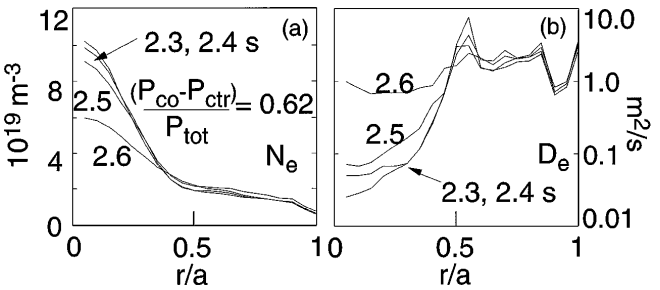

FIG. 2. (a) Profiles of the electron density at four times for a plasma that is codominated in the postlude. (b) Radial profiles of D_e for the same plasma.

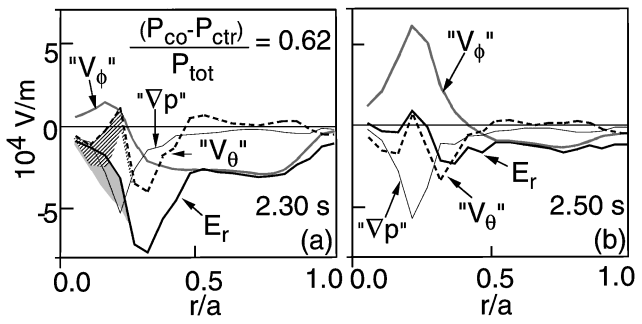

FIG. 3. (a) Radial profile of E_r for the plasma discussed in Fig. 2 and the contributions from the components of the carbon force balance equation at 2.3 s. The shaded regions represent the difference in the V_θ term and the net E_r calculated if orbit squeezing effects are ignored. (b) Same as (a), but for 2.5 s, in the early stages of confinement loss.

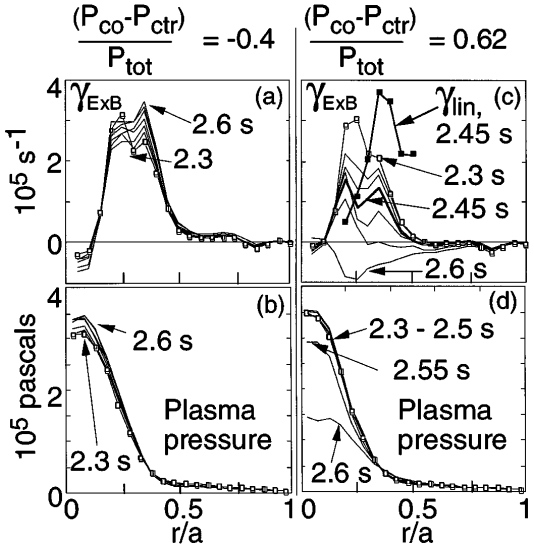

FIG. 4. Profiles of shearing rate and total plasma pressure for a counterdominated plasma (a),(b), and one of the codominated plasmas (c),(d). In the codominated case, the plasma pressure is unchanged until $\gamma_{E\times B}$ falls well below γ_{lin}^{max}.

the beam ions. Differences in E_r measured in supershots with different applied torques are consistent with V_θ being driven and damped primarily by neoclassical processes included in NCLASS [17]. However, large pressure gradients raise concern regarding violation of the usual size ordering assumed in neoclassical theory. For carbon ions, the trapped ion orbit widths are small compared to the E_r and ∇p scale lengths, so this ordering is not violated for $r/a > 0.2$, even without considering the influence of orbit squeezing [24]. Squeezing reduces the orbit size by roughly 50% for $r/a < 0.2$, preserving the ordering for all radii, and is included in the NCLASS calculations using an approximate method [25]. Since large values of dE_r/dr change the ion collisionality, the predictions of V_θ and thus E_r are modified somewhat for $r/a < 0.25$.

The pressure collapses when $\gamma_{E\times B}$ is driven by rotation below a critical value, indicating that $\mathbf{E} \times \mathbf{B}$ shear is necessary to sustain enhanced confinement (Fig. 4). The maximum linear growth rate γ_{lin}^{max} is comparable to this critical value and was calculated with a gyrofluid treatment that includes the role of Δ', but excludes the effects of $\mathbf{E} \times \mathbf{B}$ shear [26]. In these plasmas, modes are expected to become unstable primarily by the trapped electron precession resonance. In the codominated postlude plasmas, the loss of core stored energy occurs at different times but at comparable values of $\gamma_{E\times B}$, again indicating that $\mathbf{E} \times \mathbf{B}$ shear is necessary to maintain low transport (Fig. 5). The causative role of $\mathbf{E} \times \mathbf{B}$ shear is further emphasized by the fact that reductions in $\gamma_{\mathbf{E}\times\mathbf{B}}$ clearly precede back transitions, while all other plasma quantities, including Δ', are constant or nearly constant. This constancy also implies that Δ' effects alone are not sufficient to maintain enhanced confinement. However Δ' effects reduce growth rates by a factor of 2, which may be of benefit to $\mathbf{E} \times \mathbf{B}$ shear suppression.

Increases in core local fluctuation levels, measured from reflectometry [8] are correlated with increases in local transport coefficients in plasmas with back transitions (Fig. 6). Also, transport coefficients and fluctuation levels remain low until $\gamma_{\mathbf{E}\times\mathbf{B}}$ falls below the critical threshold value. The insensitivity of transport and fluctuations to variations in $\gamma_{\mathbf{E}\times\mathbf{B}}$ above a threshold value, and the similar magnitude of $\gamma_{\mathbf{E}\times\mathbf{B}}$ and γ_{lin}^{max} at the onset of increased transport and fluctuations, is consistent with

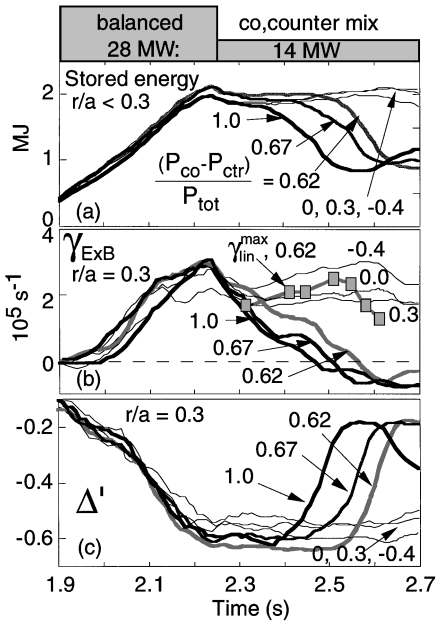

FIG. 5. (a) The stored energy, integrated out to $r/a = 0.3$ for plasmas with and without back transitions. This location is near the radius of maximum $\gamma_{\mathbf{E}\times\mathbf{B}}$ before the back transition, and is near the boundary of the region of low fluctuations (Ref. [8]). (b) $\gamma_{E\times B}$ at $r/a = 0.3$. Also shown is γ_{lin}^{max} for the codominated case with $(P_{co} - P_{ctr})/P_{tot} = 0.62$. Growth rates for the other plasmas during their 14 MW postlude ERS phases are comparable. (c) The gradient in the Shafranov shift, Δ', at $r/a = 0.3$.

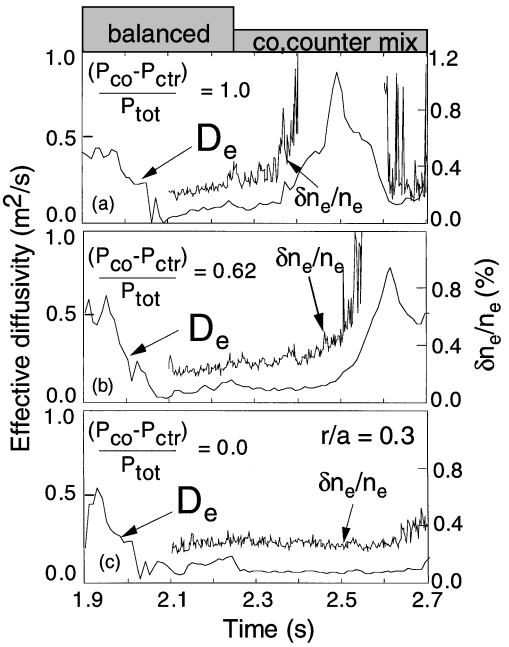

FIG. 6. The effective particle diffusivity D_e, and measured fluctuation amplitudes at $r/a = 0.3$ for plasmas with (a) all coinjection (b) predominantly coinjection $[(P_{\rm co} - P_{\rm ctr})/P_{\rm tot} = 0.62]$, and (c) balanced injection in the postlude. The measurements have spatial resolution of 1–2 cm, and sample a wave number range of $0.5 < k < 2.0$ cm^{-1}.

expectations from Ref. [12]. There, nonlinear simulations of ion drift-wave-type turbulence indicate that suppression of turbulence-induced transport should be complete when $\gamma_{\mathbf{E}\times\mathbf{B}} \sim \gamma_{\rm lin}^{\rm max}$. While the fact that $\gamma_{\rm lin}^{\rm max}/\gamma_{\mathbf{E}\times\mathbf{B}} \sim 1$–$2$ at the onset of turbulence is suggestive, the more important point is that the predicted threshold character of turbulence suppression is observed. In fact, it was suggested in Ref. [12] that parametric dependencies may influence the value of $\gamma_{\rm lin}^{\rm max}/\gamma_{\mathbf{E}\times\mathbf{B}}$ at the onset of turbulence suppression, and variations of a factor of 2 in this ratio were observed in simulations. Differences in $\gamma_{\rm lin}^{\rm max}/\gamma_{\mathbf{E}\times\mathbf{B}}$ at the transition to enhanced confinement of more than a factor of 2 were also observed in recent ERS experiments in which the B_ϕ was varied [27]. In addition, the natural turbulence decorrelation rate is the quantity more appropriately compared to $\gamma_{\mathbf{E}\times\mathbf{B}}$ [2], but it is not readily evaluated. These observations point to the need for study with respect to the identification of the most relevant shear suppression criterion.

The fluctuation amplitude increases gradually as $|\gamma_{\mathbf{E}\times\mathbf{B}}|$ decreases, suggesting that the smaller values of $|\gamma_{\mathbf{E}\times\mathbf{B}}|$ are effective in suppressing the turbulence at least partially. When transport coefficients are near a maximum, $|\gamma_{\mathbf{E}\times\mathbf{B}}|$ is near its local minimum value. For the plasma with co-only injection in the postlude [Fig. 6(a)], transport coefficients and fluctuations levels begin to fall again after 2.6 s. After this time, the $\gamma_{\mathbf{E}\times\mathbf{B}}$ profile broadens and becomes dominated by gradients in V_ϕ rather than ∇p, indicating that $\mathbf{E} \times \mathbf{B}$ shear from rotation drive may be reducing turbulence, as has been suggested for DIII-D NCS [8] and VH-mode plasmas [4].

The authors express their appreciation for the efforts and dedication of the TFTR staff. Thanks to P. H. Diamond (UCSD) for fruitful discussions, and to W. Houlberg (ORNL) for making the NCLASS code available. This work was supported by DoE Grant No. DE-AC02-76-CH-03073.

*Permanent address: Fusion Physics and Technology, Torrance, California 90503.
†Permanent address: Oak Ridge National Laboratory, Oak Ridge, Tennessee 37830.

[1] R. Taylor *et al.*, Phys. Rev. Lett. **63**, 2365 (1989).
[2] H. Biglari, P. H. Diamond, and P. W. Terry, Phys. Fluids B **2**, 1 (1990).
[3] K. Burrell *et al.*, Phys. Plasmas **1**, 1536 (1994).
[4] R. LaHaye *et al.*, Nucl. Fusion **35**, 988 (1995).
[5] F. Levinton *et al.*, Phys. Rev. Lett. **75**, 4417 (1995).
[6] E. Strait *et al.*, Phys. Rev. Lett. **75**, 4421 (1995).
[7] L. Lao *et al.*, Phys. Plasmas **3**, 1951 (1996).
[8] E. Mazzucato *et al.*, Phys. Rev. Lett. **77**, 3145 (1996).
[9] P. H. Diamond *et al.*, Phys. Rev. Lett. (to be published).
[10] M. A. Beer and G. W. Hammett, Bull. Am. Phys. Soc. **40**, 1733 (1995).
[11] J. F. Drake *et al.*, Phys. Rev. Lett. **77**, 494 (1996).
[12] R. E. Waltz *et al.*, Phys. Plasmas **1**, 2229 (1994).
[13] T. S. Hahm and K. H. Burrell, Phys. Plasmas **2**, 1648 (1995).
[14] S. Parker, Phys. Plasmas **3**, 1959 (1996).
[15] T. S. Hahm and K. H. Burrell (private communication).
[16] F. Levinton *et al.*, Phys. Rev. Lett. **63**, 2060 (1989).
[17] M. C. Zarnstorff *et al.*, Phys. Plasmas (to be published).
[18] R. Budny *et al.*, Nucl. Fusion **32**, 429 (1992).
[19] B. C. Stratton *et al.*, in *Proceedings of the IAEA Technical Committee Meeting on Time Resolved Two- and Three-Dimensional Plasma Diagnostics, Nagoya, Japan* (International Atomic Energy Agency, Vienna, 1991), p. 78.
[20] S. P. Hirshman and D. J. Sigmar, Nucl. Fusion **21**, 1079 (1981).
[21] G. Rewoldt, W. M. Tang, and R. J. Hastie, Phys. Fluids **30**, 807 (1987).
[22] N. Mattor and P. H. Diamond, Phys. Fluids **31**, 1180 (1988).
[23] M. Artun, W. M. Tang, and G. Rewoldt, Phys. Plasmas **2**, 3384 (1995).
[24] H. L. Berk and A. A. Galeev, Phys. Fluids **10**, 441 (1967).
[25] K. C. Shaing, C. T. Hsu, and R. D. Hazeltine, Phys. Plasmas **10**, 3365 (1994).
[26] M. A. Beer, Ph. D. thesis, Princeton University, 1995.
[27] F. Levinton *et al.*, in Proceedings of the Sixteenth IAEA Conference on Plasma Physics and Controlled Nuclear Fusion Research, Montreal, 1996 (International Atomic Energy Agency, Vienna, to be published).